

# SOLAR RADIATION PRESSURE AUGMENTED DEORBITING FROM HIGH ALTITUDE SUN-SYNCHRONOUS ORBITS

**Charlotte Lücking, Camilla Colombo, Colin McInnes**

*Advanced Space Concepts Laboratory  
University of Strathclyde, Glasgow G1 1XJ, UK  
charlotte.lucking@strath.ac.uk*

## ABSTRACT

This paper discusses the use of solar radiation pressure (SRP) augmented deorbiting to passively remove small satellites from high altitude Sun-synchronous orbits. SRP-augmented deorbiting works by deploying a light-weight reflective inflatable device to increase the area-to-mass-ratio of the spacecraft. The interactions of the orbital perturbations due to solar radiation pressure and the Earth's oblateness cause the eccentricity of the orbit to librate at a quasi-constant semi-major axis. A large enough area-to-mass-ratio will ensure that a maximum eccentricity is reached where the spacecraft will then experience enough aerodynamic drag at the orbit pericentre to deorbit. An analytical model of the orbital evolution based on a Hamiltonian approach is used to obtain a first guess for the required area-to-mass-ratio to deorbit. This first guess is then used in a numerical propagation of the orbital elements using the Gauss' equations to find the actual requirements as a function of altitude. The results are discussed and altitude regions for Sun-synchronous orbits are identified in which the proposed method is most effective. Finally, the implementation of the device is discussed. It is shown that passive solar radiation pressure deorbiting is a useful alternative to propulsive end-of-life manoeuvres for future high altitude Sun-synchronous missions.

## 1 INTRODUCTION

In 1993 the Inter-Agency Space Debris Coordination Committee was formed and issued guidelines for the mitigation of space debris which demands a removal of any spacecraft from certain protected regions within 25 years after the end of operations [1]. The most congested orbits are Sun-synchronous orbits (SSO). These are high inclination, retrograde Low Earth Orbits (LEO) with a progression of the line of nodes due to planetary oblateness which matches the precession of the Sun-line due to the Earth's motion around the Sun. The orbit plane thus keeps the same orientation with respect to the Sun. The most popular SSOs are dawn/dusk and noon/midnight orbits. The latter offer favourable lighting conditions with short shadows throughout the year. Dawn/dusk orbits are eclipse-free.

The most conventional methods approaches to orbit removal are passive orbit decay due to drag and a propulsive end-of-life manoeuvre. Without the use of drag-augmenting structures, the former only works in lower LEO orbits. Propulsive methods can pose problems for small satellites which often do not incorporate a propulsion system. Clearly, they also require more propellant the higher the orbit altitude and can quickly become infeasible for low specific impulse thrusters.

Passive deorbiting technologies which have previously been suggested either make use of aerodynamic [2-5] or electrodynamic drag forces [6-8]. Drag augmented deorbiting (DAD) works by increasing the spacecraft area-to-mass-ratio and thus increasing the rate of loss of orbital energy

due to atmospheric drag. Electrodynamic Tethers (EDT) are deployable conductive tethers. The movement of the EDT through the Earth's magnetic field induces a current in the tether. The current results in a Lorentz force, which alters the orbital energy over time. Both effects decrease rapidly with increasing distance from the Earth. DAD is not feasible for altitudes beyond about 1000 km. EDTs are dependent on the Earth's magnetic field and are sensitive to initial orbital inclination. They work best in equatorial orbits and decrease in efficiency with increasing inclination and are unreliable above 75 degrees. Thus, neither method is applicable to high altitude Sun-synchronous orbits.

SRP-augmented deorbiting can provide a passive end-of-life solution for these orbits. Akin to the DAD method, a large reflective deployable structure is used to increase the spacecraft area-to-mass-ratio. Then, the combined effects of SRP and the  $J_2$  perturbation cause an increase in orbital eccentricity to lower the orbit perigee and so induce air drag. SRP-augmented deorbiting was initially introduced as an analytical solution for planar orbits [9]. The analytical model which neglects the obliquity of the equator over the ecliptic has then been verified numerically and extended to inclined Medium Earth Orbits (MEO) [10]. This paper focuses on the feasibility of the strategy for deorbiting high altitude Sun-synchronous orbits. For this problem a new specialised analytical model is derived and then compared to numerical solutions. First, however, a summary of the previous work on SRP-augmented deorbiting is given.

## 2 SRP-AUGMENTED DEORBITING

SRP-augmented de-orbiting exploits the effect of solar radiation pressure (SRP) and Earth oblateness in combination with aerodynamic drag to passively de-orbit a satellite within a given time after the end-of-life. This is achieved by making use of the interaction between the SRP and  $J_2$  effect to increase the eccentricity of an initially circular in-plane orbit until the perigee reaches an altitude at which the aerodynamic drag causes the spacecraft to de-orbit. The orbital evolution can be divided into two phases as visualised in Figure 1.

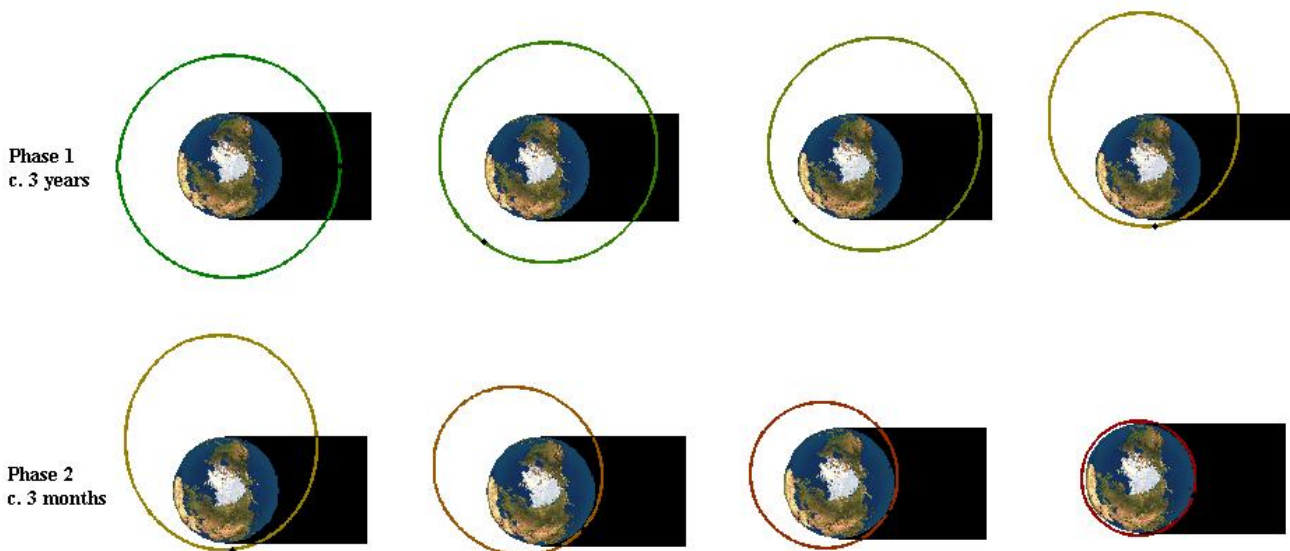


**Figure 1:** The two phases of the de-orbiting manoeuvre. In this example the initial orbit altitude was 7000 km and the effective are-to-mass-ratio  $3 \text{ m}^2/\text{kg}$ .

The first phase takes up about 90% of the total manoeuvre time. In phase one, solar radiation pressure is dominant over drag and is exploited to increase the orbit eccentricity at a quasi-constant semi-major axis until drag becomes the dominant force. Then phase 2 begins in which aerodynamic

drag decreases the orbital energy, and thus the semi-major axis of the spacecraft, and the eccentricity at the same time so that the perigee altitude is kept near constant. In the very last period of the manoeuvre the orbit is quasi-circular and at an altitude where drag decreases the orbit altitude rapidly. At this stage the device acts in the same way as drag-augmenting devices would. Solar radiation pressure is at this point negligible compared to the drag force.

SRP-augmented deorbiting was first investigated analytically using a Hamiltonian  $H_{planar}$  expressing the orbital evolution due to SRP and the  $J_2$  effect for equatorial orbits, when the tilt of the Earth's rotational axis with respect to the ecliptic normal is neglected.

$$H_{planar}(e, \phi) = \alpha e \cos \phi - \frac{\kappa}{3\sqrt{1-e^2}} - \sqrt{1-e^2} \quad (1)$$

This expression was presented in reference [11] and it uses three parameters to describe an orbit: semi-major axis  $a$ , eccentricity  $e$ , and  $\phi$ , the angle between the direction of solar radiation and the orbit's perigee as seen from the centre of the Earth. Apart from the orbital parameters it is also dependant on the solar radiation pressure parameter  $\alpha$  and the  $J_2$  effect parameter  $\kappa$ .

$$\alpha = \frac{3F_{\odot}}{2n_{\odot}c} c_R \sigma \sqrt{\frac{a}{\mu}} \quad (2)$$

$$\kappa = \frac{3}{2n_{\odot}} J_2 R_E^2 \sqrt{\frac{\mu}{a^7}} \quad (3)$$

where  $n_{\odot}$  is the orbit rate of the Earth around the Sun,  $F_{\odot}$  is the solar radiation flux at Earth,  $c$  is the speed of light in vacuum,  $\mu$  is the gravitational parameter of the Earth,  $J_2$  the second zonal harmonic coefficient of the Earth and  $R_E$  the Earth's mean radius. The defining spacecraft characteristic for the solar radiation pressure parameter is the effective area-to-mass-ratio  $c_R \sigma$ , the product of  $c_R$ , the coefficient of reflectivity, and  $\sigma$ , the area-to-mass-ratio. The coefficient of reflectivity depends on the optical properties for the device and its geometry.

Using the Hamiltonian, equations were derived in reference [9] to calculate the minimum required area-to-mass-ratio to deorbit from a circular planar orbit of a given semi-major axis. These equations were validated against a numerical simulation in reference [10] in which the simplifying assumption of zero obliquity angle between the equator and the ecliptic was dropped. It was shown that the analytical expressions were reasonably accurate at predicting the behaviour for low inclination orbits. However, at higher inclinations they became ever more unreliable. A modified analytical approach is needed to investigate the application of SRP-augmented deorbiting to Sun-synchronous orbits.

### 3 ANALYTICAL MODEL

In order to assess the problem analytically some assumptions and simplifications have to be made. As already assumed in equation (1), the tilt of the Earth's axis and the effect of eclipses are neglected. Furthermore, out-of-plane effects are not considered in the analytical SRP model. Therefore, the predicted behaviour will be most accurate for a noon/midnight orbit, as this orbit predominantly faces the Sun edge on and thus experiences only small SRP forces along the normal of the orbital plane (Figure 2a). Dawn/dusk orbits however experience mainly out-of-plane forces (Figure 2b).

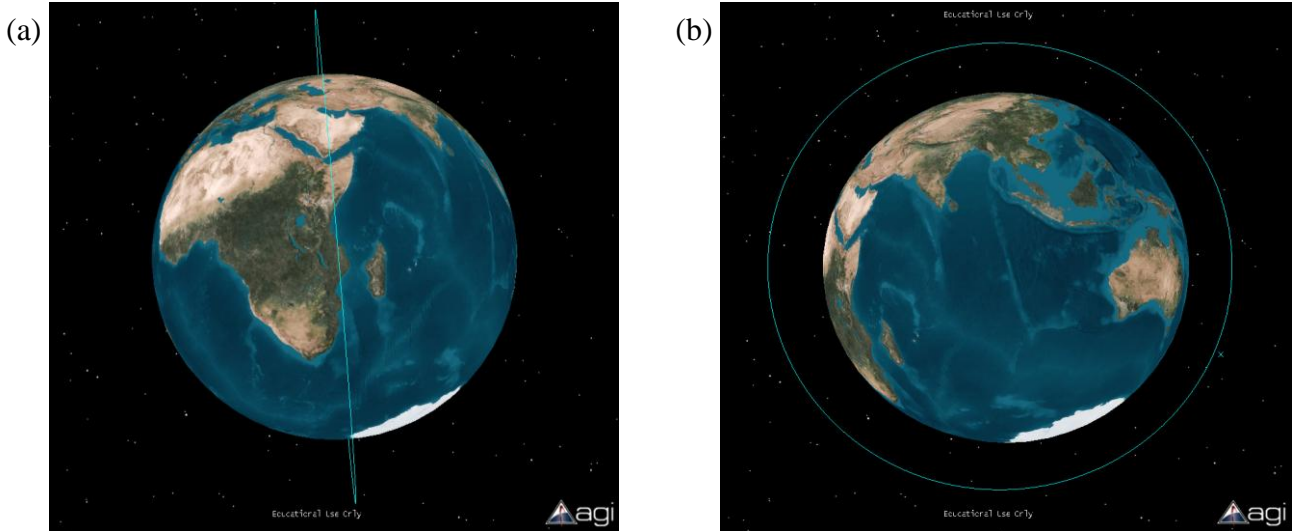


**Figure 2:** Sun-synchronous orbits: (a) noon/midnight orbit, (b) dawn/dusk orbit as seen from the direction of the Sun.

The first step in the creation of a modified analytical model is to look at the components of the Hamiltonian for planar orbits in equation (1). The first term represents for the effect of solar radiation pressure and is dependent on the SRP parameter  $\alpha$ . The second term represents the effect of the Earth's oblateness and is dependent on the  $J_2$  effect parameter  $\kappa$ . The final term represents the precession of the Earth around the Sun.

For Sun-synchronous orbits the SRP term remains the same because we are neglecting out-of-plane forces. Sun-synchronous orbits are designed in such a way as to cancel out precession of the Earth around the Sun and the change in the line of nodes due to the  $J_2$  effect. This means that  $\dot{\phi} = \dot{\omega}$ . Thus, the last term of equation (1) can be removed so that the second term only needs to consider the change in the argument of perigee. The modified Hamiltonian can be written as:

$$H_{sync}(e, \omega) = \alpha e \cos \omega - \frac{\kappa_{sync}}{3\sqrt{1-e^2}} \quad (4)$$

with

$$\kappa_{sync} = \frac{d\omega}{dt} \frac{(1-e^2)^2}{n_{\odot}} = \frac{3}{2n_{\odot}} J_2 R_E^2 \sqrt{\frac{\mu}{a^7}} \left( 2 - \frac{5}{2} \sin i_{sync} \right) \quad (5)$$

The Sun-synchronous inclination  $i_{sync}$  for circular orbits can be calculated for a given semi-major axis using the following expression:

$$\cos i_{sync} = -\frac{n_{\odot}}{3J_2 R_E^2} \sqrt{\frac{a^7}{\mu}} \quad (6)$$

With this term the following expression for  $\kappa_{sync}$  can be found:

$$\kappa_{sync}(a) = 3 \sqrt{\frac{J_2^2 R_E^4 \mu}{n_{\odot}^2 a^7}} - \frac{15}{4} \sqrt{\frac{J_2^2 R_E^4 \mu}{n_{\odot}^2 a^7} - \frac{4}{9}} \quad (7)$$

Next, the required area-to-mass-ratio for deorbiting is derived in a way analogous to reference [9]. The value of the Hamiltonian for a circular orbit is calculated by setting the eccentricity to zero in equation (4):

$$H_{sync}(e=0) = \frac{\kappa_{sync}}{3} \quad (8)$$

The Hamiltonian equation (4) is then set equal to equation (8) in order to isolate the phase line in the orbital element phase space of eccentricity  $e$  and argument of perigee  $\omega$  which passes through  $e = 0$ . As previous work has shown, the maximum eccentricity can only be reached at either  $\omega = 0$  or  $\omega = \pi$  [9]. Thus, using equation (2) the following expression for the required effective area-to-mass-ratio  $c_R\sigma$  can be found:

$$c_R\sigma(a) = 2 \frac{n_{\odot}c}{F_{\odot}} \sqrt{\frac{\mu}{a}} \left( 1 - \sqrt{1 - (1 - R_E a^{-1})^2} \right)^{-3} \frac{\kappa_{sync}(a)}{(1 - R_E a^{-1})} \quad (9)$$

The results of the analytical approach are represented in Figure 3. They are similar to those for planar orbits presented in reference [9], but the location of the minimum is at 4300 km rather than 7500 km as in the planar case.

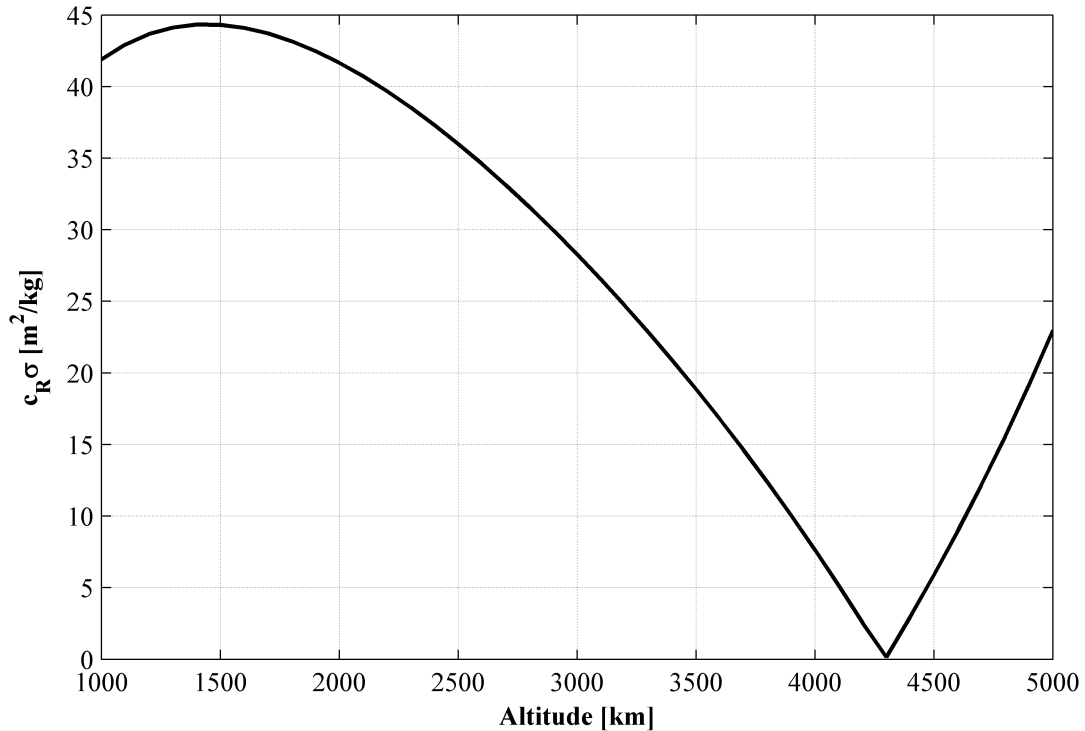


**Figure 3:** The analytical results for the required effective area-to-mass-ratio  $c_R\sigma$  to deorbit a Sun-synchronous orbit of given altitude.

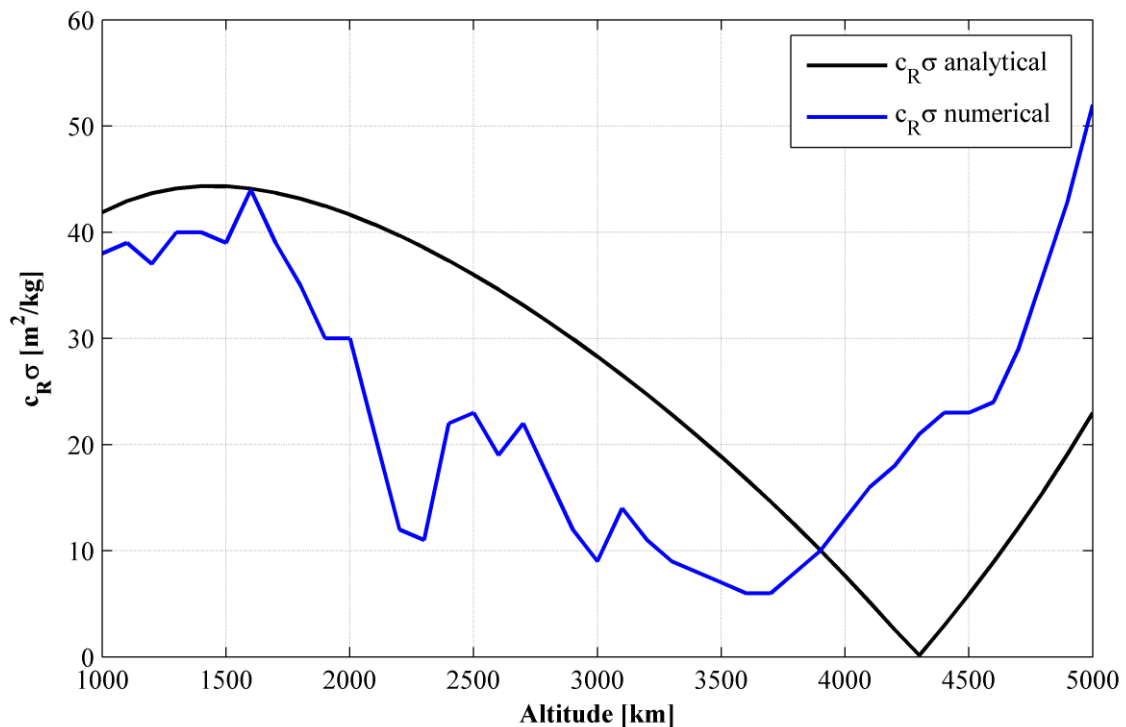
In the next section the analytical results are compared to numerical solution. It is not expected that the analytical prediction is very accurate as several simplifications and assumptions had to be made. In particular, the out-of-plane forces due to SRP were neglected. This assumption is most accurate for noon/midnight orbits but not even for these is the orbit normal permanently orthogonal to the solar radiation. Due to the tilt of the Earth's axis, the aspect angle with respect to the Sun oscillates

over the year. Neither is the assumption that the orbits are Sun-synchronous throughout the orbital evolution accurate. As soon as the eccentricity begins to increase the Sun-synchronous inclination changes and a progression of the line of nodes sets in.

#### 4 NUMERICAL ANALYSIS

In this model, the orbital dynamics are propagated numerically by integrating the Gauss' equations in non-singular Lagrangian elements in MATLAB [12]. The use of those equations and the validity of the  $e$ - $\phi$  phase space for inclined orbits has been analysed in [13]. The numerical propagation considers only the perturbations of solar radiation pressure and the  $J_2$  effect. The drag effect and eclipses are neglected to save in computational time. The criterion for a successful deorbit is a perigee altitude of zero and the maximum propagation time is set to five years.

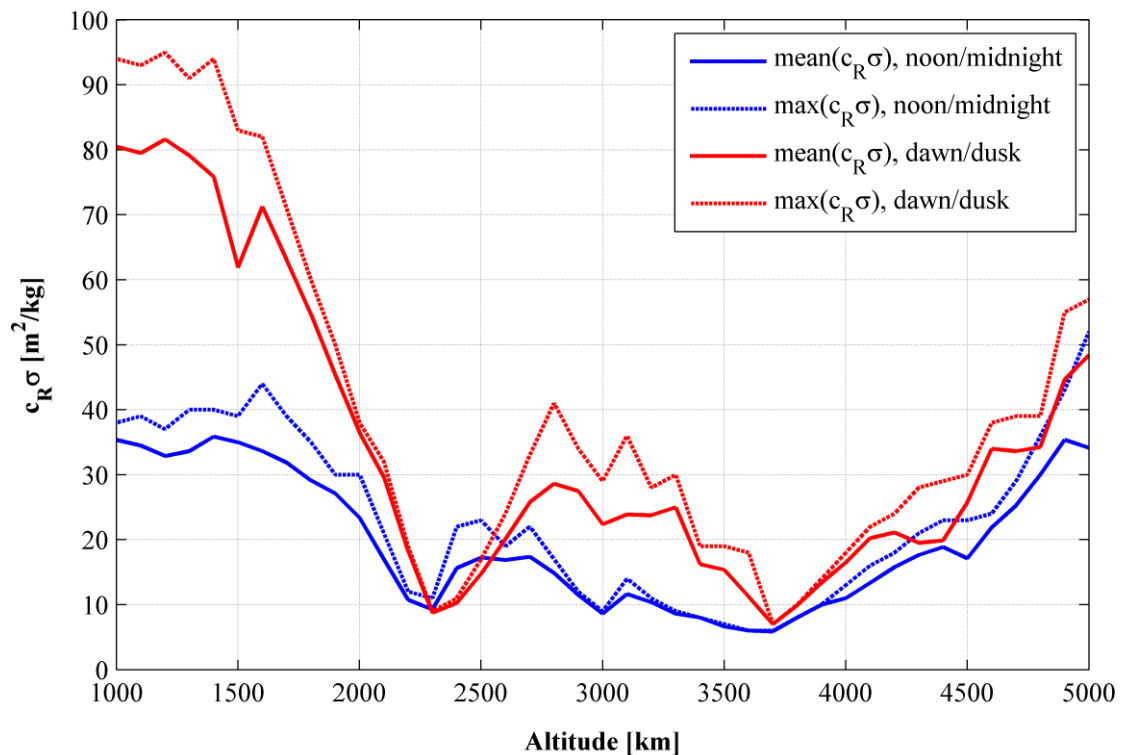
In order to find the required effective area-to-mass-ratio, a numerical search was implemented. The scenario was simulated starting from the analytical best guess for  $c_R\sigma$  from equation (9) and, depending on whether the deorbit was successful or not, a higher or lower  $c_R\sigma$  was chosen for the next run. This was continued until the required  $c_R\sigma$  was determined within an accuracy of  $1 \text{ m}^2/\text{kg}$ . The results for maximum area-to-mass required for deorbiting noon/midnight orbits compared to the analytical prediction are shown in Figure 4. It can be seen that, as expected, the analytical model is not very accurate. However, the general magnitude of the results was right and also the v-shaped trend is noticeable. The minimum occurs at an altitude a 600 km lower than predicted by the simple analytical model.



**Figure 4:** Analytical (black) and numerical (blue) results for the required effective area-to-mass-ratio to deorbit a Sun-synchronous noon/midnight orbit of a given altitude.

Using the method described above the required effective area-to-mass-ratio for deorbit was calculated for a range of initial altitudes and local times of the ascending node. For each case the result was found for eight different starting dates equally spread throughout the year starting from

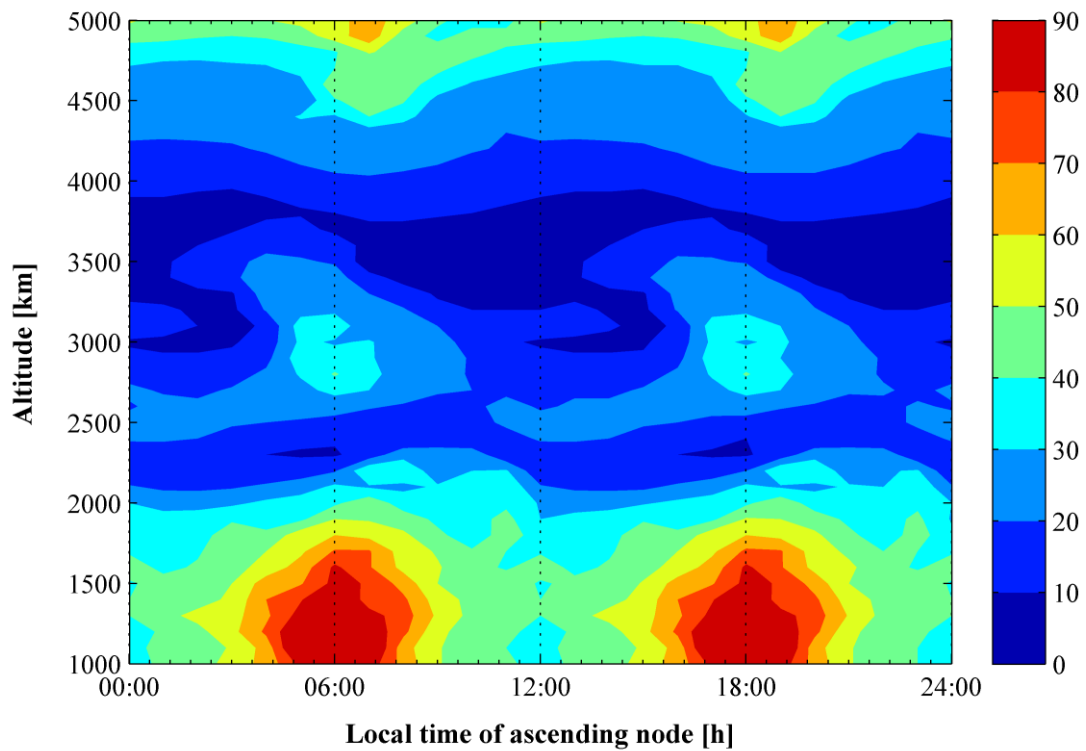
the spring equinox. The mean and maximum results for noon/midnight and dawn/dusk orbits are shown in Figure 5. As expected the method is less effective for dawn/dusk orbits than for noon/midnight orbits at lower altitudes because out of plane forces are higher for dawn/dusk orbits. However, this difference in area-to-mass-ratio shrinks for increasing altitude. This is due to fact that the Sun-synchronous inclination increases with larger altitudes, and thus the orbital plane becomes more aligned with the equator. This means that even dawn/dusk orbits will experience stronger in-plane SRP effects.



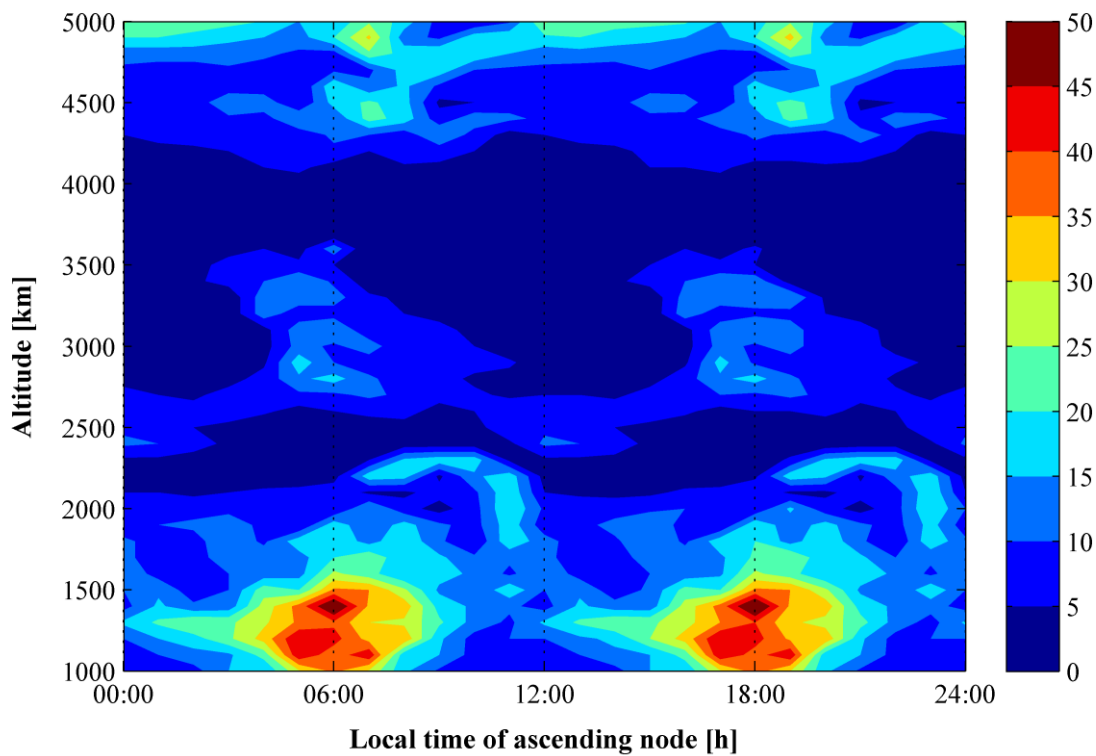
**Figure 5:** Numerical results for the mean (solid) and maximum (dashed) required effective area-to-mass-ratio to deorbit from a noon/midnight (blue) or dawn/dusk (red) Sun-synchronous orbit for different initial altitudes.

Figure 6 shows the required effective area-to-mass-ratio for all Sun-synchronous orbits altitudes between 1000 km and 5000 km. The result shown is the maximum for the different manoeuvre starting times throughout the year. The greatest difference between starting at different times is experienced by dawn/dusk orbits of altitudes between 1000 km and about 1500 km. In this region the results can vary by up to 50 m<sup>2</sup>/kg (see Figure 7). The required effective area-to-mass-ratio is lowest for 6:00h orbits when the manoeuvre starts in autumn and symmetrically lowest for 18:00h orbits when the manoeuvre starts in spring.

It can be seen from both figures that SRP-augmented deorbiting is most effective and reliable for Sun-synchronous orbits with semi-major axes between about 2000 km and 4500 km. In this region the maximum required effective area-to-mass-ratio is mainly below 20 m<sup>2</sup>/kg and always below 40 m<sup>2</sup>/kg. The sensitivity to the starting date of the manoeuvre is also low. This is an advantage when a fail-safe deorbiting mechanism is applied. This is a design which automatically deploys when the satellite's main electronics are dead in order to avoid a failure of the end-of-life system. With systems which are deployed on command from ground this characteristic is irrelevant as the operator can simply wait until the best time to start the deorbiting manoeuvre.



**Figure 6:** Contour plot of the numerical results for the maximum required effective area-to-mass-ratio in  $\text{m}^2/\text{kg}$  for Sun-synchronous orbits of different altitude and local time of ascending node.



**Figure 7:** Contour plot of the maximum difference in required effective area-to-mass-ratio in  $\text{m}^2/\text{kg}$  for Sun-synchronous orbits of different altitude and local time of ascending node depending on the time of the year the manoeuvre is initiated.

## 5 VERIFICATION

In this section the numerical results presented in the previous section are verified using Satellite Tool Kit (STK v9.2.2). This is necessary to test the assumption that perturbations other than SRP and the  $J_2$  effect and eclipses can be neglected when performing a rough analysis of SRP-augmented deorbiting. The propagation in STK was performed with the HPOP propagator and including aerodynamic drag, the Earth gravitational harmonics up to 21<sup>st</sup> order, and third body perturbations by the Sun and the Moon in addition to SRP and the  $J_2$  effect. Three different scenarios were tested (see Figure 8).

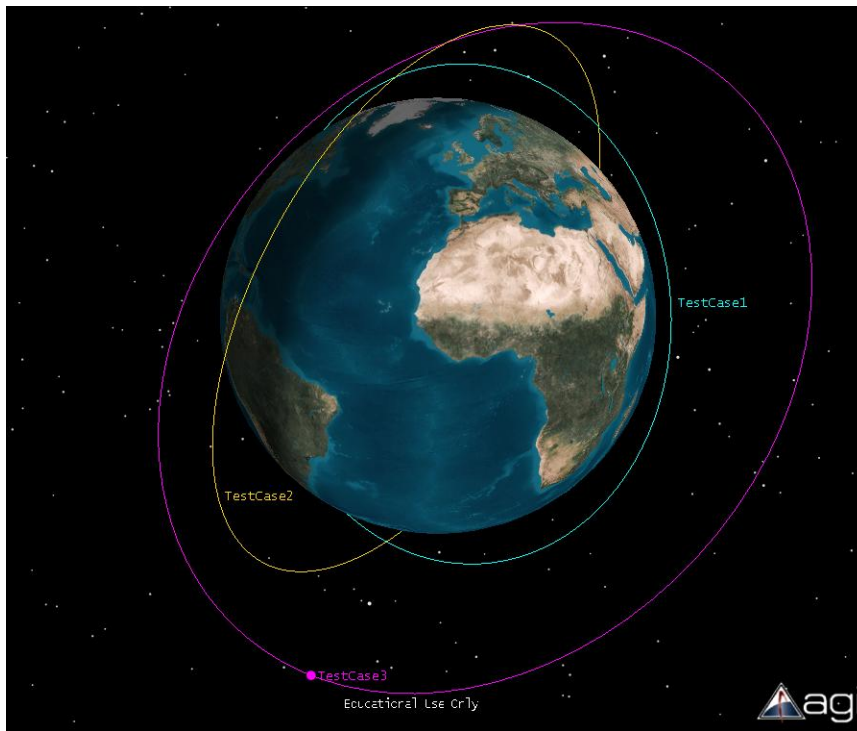


**Figure 8:** The three test case Sun-synchronous orbits with different initial altitudes and local times of the ascending node.

### 5.1 Low altitude test case

For the first test case a noon/midnight Sun-synchronous orbit with an altitude of 1000 km was chosen. The results of the numerical model predict a required effective area-to-mass-ratio of 35 m<sup>2</sup>/kg for this orbit. When a spacecraft with these characteristics is propagated in STK it deorbits within only two months. This is due to the strong effect of drag which was neglected in the numerical model but which affects a spacecraft of the given area-to-mass-ratio even at 1000 km altitude. To verify the same simulation was run without the effect of SRP and a similar deorbit time was recorded.

To assess by how much the area-to-mass-ratio can be decreased owing to aerodynamic drag the scenario was run again with area-to-mass-ratios of 15 m<sup>2</sup>/kg, 5 m<sup>2</sup>/kg and 1 m<sup>2</sup>/kg. The deorbiting was successful within 5 years for the first two cases and unsuccessful for the last. In the case of the 5 m<sup>2</sup>/kg spacecraft the manoeuvre was completed within 500 days. Figure 9a shows the results for the perigee altitude and the semi-major axis throughout the manoeuvre. The effect of SRP which causes the eccentricity to librate can be seen in the periodic variation in perigee altitude while the decline in semi-major axis is more uniform. The same simulation was then run again, neglecting solar radiation pressure. In this case the spacecraft did not deorbit within the same time span as can be seen in Figure 9b.

The evolution of the altitude as seen in Figure 9a is not nearly strong enough to bring the perigee down into the lower atmosphere or to a zero altitude as required in the MATLAB simulation. But it is enough to periodically increase the effect of drag and thus speed up the final decay. This means that for the lower altitudes the numerical model overestimates the required effective area-to-mass-ratio.

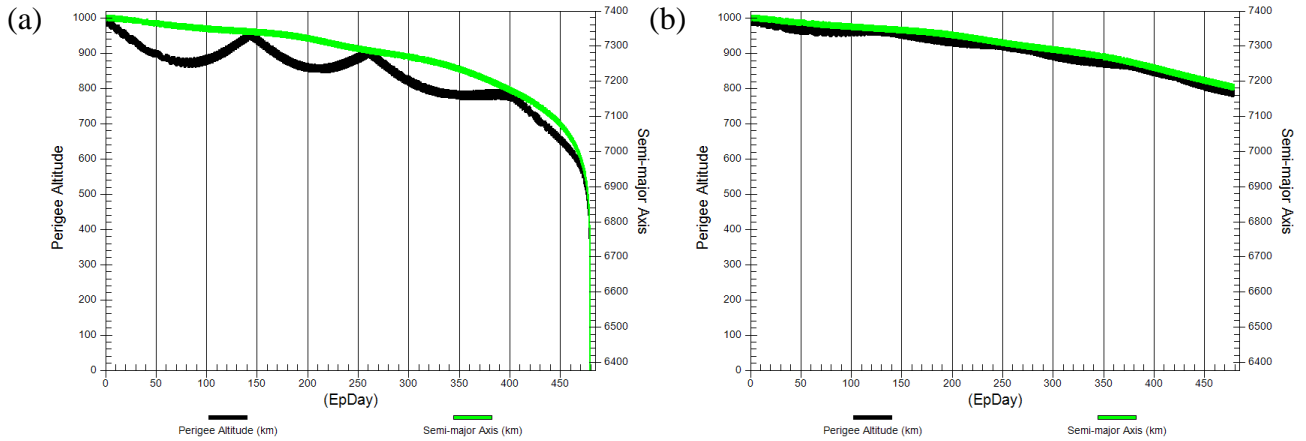


**Figure 9:** Evolution of the perigee altitude (black) and semi-major axis (green) of a 1000 km noon/midnight Sun-synchronous orbit for a spacecraft with an effective area-to-mass-ratio of  $5 \text{ m}^2/\text{kg}$  including the effect of SRP (a) and excluding the effect of SRP (b) computed with HPOP in STK v9.2.2.

## 5.2 Medium altitude test case

For the next test case a 2300 km dawn/dusk orbit was chosen. At this altitude the required area-to-mass-ratio shows a local minimum for dawn/dusk orbits. The predicted required effective area-to-mass-ratio was  $10 \text{ m}^2/\text{kg}$ . Propagating this scenario shows that as predicted a successful deorbiting manoeuvre is completed within 3.5 years (see Figure 10a).

Again this result is compared to a simulation in which solar radiation pressure is neglected. In this case drag has a minimal effect on the orbit evolution (see Figure 10b). In this figure the slight oscillations in perigee altitude are due to third body effects. For this scenario the numerical prediction is accurate and the effect of solar radiation pressure is essential to the eventual re-entry.

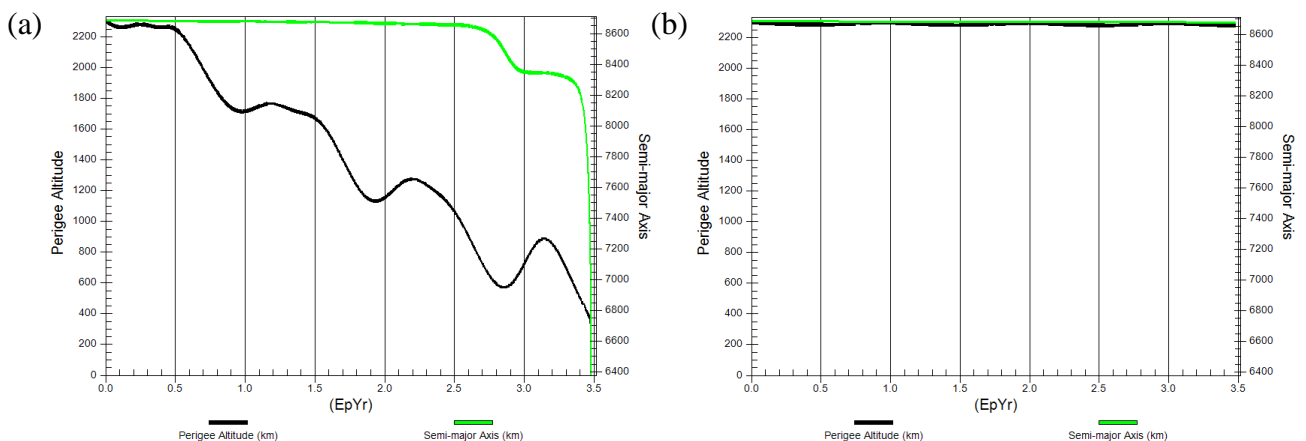


**Figure 10:** Evolution of the perigee altitude (black) and semi-major axis (green) of a 2300 km dawn/dusk Sun-synchronous orbit for a spacecraft with an effective area-to-mass-ratio of  $10 \text{ m}^2/\text{kg}$  including the effect of SRP (a) and excluding the effect of SRP (b) computed with HPOP in STK v9.2.2.

### 5.3 High altitude test case

For the final test case a 4000 km noon/midnight orbit was chosen. The predicted required effective area-to-mass-ratio for this scenario is  $15 \text{ m}^2/\text{kg}$  maximum. The simulation in STK shows that this prediction is justified. The manoeuvre is completed within one year (see Figure 11a). A comparison to the simulation without SRP shows again that the effect of solar radiation pressure is instrumental in the manoeuvre as the semi-major axis and eccentricity hardly vary at all in the latter case (see Figure 11b).

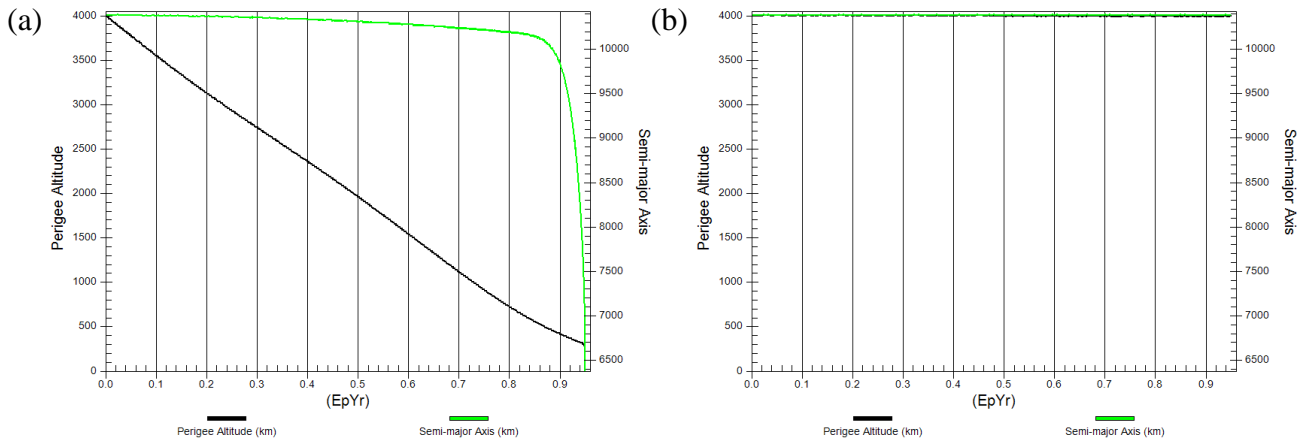


**Figure 11:** Evolution of the perigee altitude (black) and semi-major axis (green) of a 4000 km noon/midnight Sun-synchronous orbit for a spacecraft with an effective area-to-mass-ratio of  $15 \text{ m}^2/\text{kg}$  including the effect of SRP (a) and excluding the effect of SRP (b) computed with HPOP in STK v9.2.2.

## 6 DESIGN IMPLEMENTATION

In this section possible implementations of SRP-augmented deorbiting are discussed. In the first part different basic design options are examined. In the second part the technology development efforts at the University of Strathclyde are presented and conclusions for the feasibility of an SRP-augmented deorbiting device for CubeSats drawn from them.

### 6.1 Basic design options for deorbiting device

The main options for the shape of the device are a balloon, a cone/pyramid or a flat sail. Of these only the balloon is truly passive. The cone and the sail would need to be directed to face the Sun in order to experience the desired effect on the orbit evolution. However, the balloon would also need eight-times more surface material than the sail. This is due to the ratio of surface area of a sphere to its cross-sectional area and because of the reflection characteristics of a sphere. While a fully reflective, flat sail oriented normal to the incident Sunlight will have an effective coefficient of reflectivity of 2, a sphere will only have an effective coefficient of reflectivity of 1 and thus needs double the cross-sectional area.

This effect is caused by the direction of the reflected light. While the radiation in the middle of the sphere is reflected back towards the Sun, the angle of reflection changes towards the edge of the sphere. When all impulses are integrated over the whole cross-section of the sphere an effective coefficient of reflectivity of 1 is found, regardless of the reflectivity of the surface material as long as it is not transmissive. For a cone the effective coefficient of reflectivity depends on the cone angle. A shallow cone will receive a larger impulse from the solar radiation than a steep one.

The advantage of a sphere is that it has the same cross-sectional area from any aspect angle. Thus, after deployment and rigidisation no further control is needed. The manoeuvre will occur

completely passively. A flat sail would need to be controlled in order to constantly face the Sun. This is similar to solar sailing. However, a simpler control algorithm can be implemented because no orbit propagation needs to be performed on-board and the only condition is to keep the sail Sun-pointing. Another advantage over conventional solar sailing is that no fast attitude changes need to be performed.

A cone or pyramid is a compromise between the balloon and the sail. It requires a medium amount of surface material and due to its conic shape experiences the shuttlecock effect which creates an oscillation around the equilibrium attitude. A cone design would need a mechanism to dampen this oscillation. Then a constantly Sun-pointing attitude could be assured for altitudes outside the zone where aerodynamic drag could be felt.

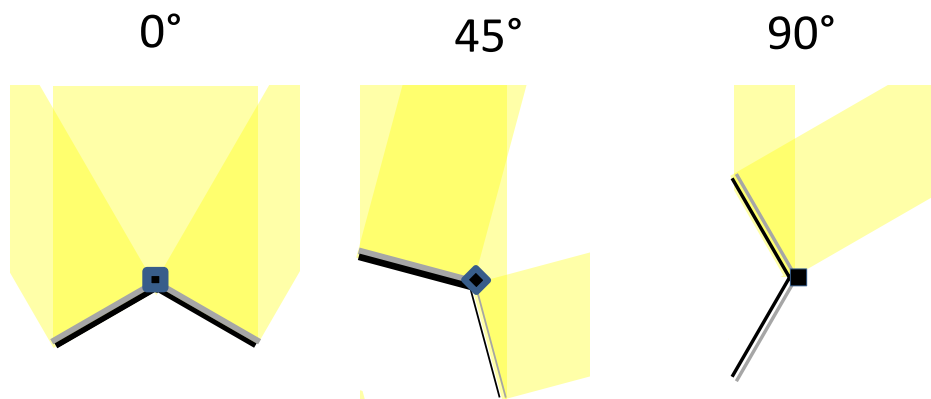


**Figure 12:** Different pitch angles for a reflective cone/pyramid under the influence of solar radiation pressure [14].

A problem for the sail and the cone also arises when the spacecraft enters the drag zone. In this region the force of drag and the force of SRP can act from different directions. The cone would naturally face the combined force vector. The sail would be harder to control. If it continues to be Sun-pointing the evolution might differ from the one calculated in this paper.

## 6.2 Development of a foldable pyramid for CubeSat deorbiting (FRODO)

FRODO, the Foldable Reflective system for Omniaitude DeOrbiting a deployable pyramid system for passive deorbiting which is currently under development at the University of Strathclyde. A team of students is sponsored by the European Space Agency to partake in the current REXUS sounding rocket mission. Their experiment consists of two ejectable CubeSat modules which will carry novel deployable space structures for testing in near vacuum milligravity conditions. One of these experiments is FRODO [15].

The residual air inflation method is used to deploy the device. During assembly in ambient pressure air is trapped within the sealed elements of the structure. In reduced pressure conditions this air causes the structure to deploy. A first model of the pyramid was manufactured out of 12  $\mu\text{m}$  thick aluminium coated polyester foil using 30  $\mu\text{m}$  layflat polythene for the strut elements. The resulting structure measured 1.78x1.78x0.51  $\text{m}^3$  giving an effective area-to-mass-ratio of 5  $\text{m}^2/\text{kg}$  to a 1 kg CubeSat (see Figure 13a). The whole pyramid could be stowed inside a 10x10x2  $\text{cm}^3$  volume achieving a packaging efficiency of about 50% (see Figure 13b). In future iterations mass savings can be made by using thinner Mylar (5  $\mu\text{m}$ ) for the surface of the structure and reducing the pyramid height. A quick calculation shows that using the Mylar and 20 degree slopes on the pyramid an effective area-to-mass-ratio of 20  $\text{m}^2/\text{kg}$  can be achieved with 30% of a 1U CubeSat volume.

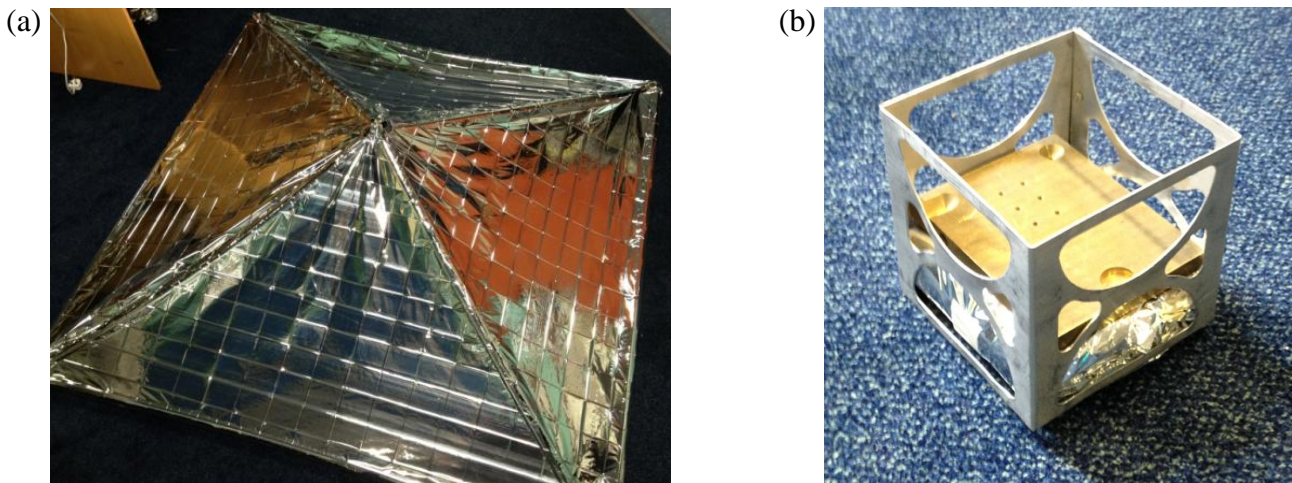


**Figure 13:** FRODO, the Foldable Reflective system for Omnialtitude DeOrbiting, deployed offering 5 m<sup>2</sup>/kg of effective area-to-mass-ratio for a 1 kg CubeSat (a) and stowed inside the CubeSat structure (b) [14].

## 7 CONCLUSIONS

SRP-augmented deorbiting has been shown to be an effective method to passively deorbit spacecraft from high altitude Sun-synchronous orbits. For orbits with altitudes around 1000 km it will speed up the orbital decay due to aerodynamic drag by causing the eccentricity to oscillate. For higher altitudes solar radiation pressure is the dominating factor in the deorbiting manoeuvre. SRP-augmented deorbiting is most effective for Sun-synchronous orbits of altitudes between 2000 km and 4500 km. Simulations run which neglected SRP effects showed only very minor variations in semi-major axis and eccentricity. Moreover, deorbiting simulation performed through STK allowed validating the analytical model which considered only SRP and  $J_2$  effect. Different design options for a SRP-augmentation device were discussed. A balloon-type device would be truly passive while a cone or a sail offer a larger cross-sectional area in relation to surface material used. Technology developments at the University of Strathclyde show that a pyramid-shaped device can supply 20 m<sup>2</sup>/kg effective area-to-mass-ratio when packed into 30% of the spacecraft volume.

## ACKNOWLEDGMENTS

This work was funded by the European Research Council grant 227571 (VISIONSPACE). The validation was performed with Satellite Tool Kit. The educational license was kindly supplied by Analytical Graphics, Inc. (AGI). The main author's attendance at the 4S Symposium 2012 was funded by the IET Travel Grant and the Symposium Committee. Charlotte Lücking is also supported by the IET Hudswell International Scholarship 2011 and the Frank J. Redd Student Scholarship.

## REFERENCES

- [1] IADC Space Debris Mitigation Guidelines, IADC Document No. IADC-02-01, 15 October 2002, Revision 1, September 2007.
- [2] P. C. E. Roberts, P. G. Harkness, Drag Sail for End-of-Life Disposal from Low Earth Orbit, *Journal of Spacecraft and Rockets*, 44 (6), pp. 1195-1203, 2007. doi: 10.2514/1.28626

- [3] D. C. Maessen, E. D. v. Breukelen, B. T. C. Zandbergen, O. K. Bergsma, Development of a Generic Inflatable De-orbit Device for CubeSats, Paper No. IAC-07-A6.3.6, presented at the 58<sup>th</sup> International Astronautical Congress, Hyderabad, India, 24 - 28 September 2007.
- [4] K.T. Nock, K.L. Gates, K.M. Aaron, A.D. McDonald, Gossamer Orbit Lowering Device (GOLD) for Safe and Efficient De-orbit, Paper No. AIAA-2010-7824, presented at the AIAA Astrodynamics Specialists Conference, Toronto, Canada, 2 - 5 August 2010.
- [5] J. Andrews, K. Watry, K. Brown, Nanosat Deorbit and Recovery System to Enable New Missions, Paper No. SSC11-X-3, presented at the 25th AIAA/USU Conference on Small Satellites, Logan, Utah, USA, 8 - 12 August 2011.
- [6] L. Iess, C. Bruno, C. Ulivieri, U. Ponzi, M. Parisse, G. Laneve, G. Vannaroni, M. Dobrowolny, F. De Venuto, B. Bertotti, L. Anselmo, Satellite de-orbiting by means of electrodynamic tethers part I: General concepts and requirements, *Acta Astronautica*, 50, pp. 399-406, 2002.  
doi: 10.1016/S0094-5765(01)00180-1
- [7] L. Iess, C. Bruno, C. Ulivieri, G. Vannaroni, Satellite de-orbiting by means of electrodynamic tethers part II: System configuration and performance, *Acta Astronautica*, 50, pp. 407-416, 2002.  
doi: 10.1016/S0094-5765(01)00181-3
- [8] R. L. Forward, R. P. Hoyt, Terminator Tether(TM): A spacecraft deorbit device, *Journal of Spacecraft and Rockets*, 37 (2), pp. 187-196, 2000.  
doi: 10.2514/2.3565
- [9] C. Lücking, A Passive High Altitude Deorbiting Strategy, Paper No. SSC11-VIII-6, presented at the 25<sup>th</sup> AIAA/USU Conference on Small Satellites, Logan, Utah, USA, 8 - 12 August 2011.
- [10] C. Lücking, C. Colombo, and C. R. McInnes, "A Passive Satellite Deorbiting Strategy for Medium Earth Orbits Using Solar Radiation Pressure and the  $J_2$  Effect," accepted for publication in *Acta Astronautica*, 2012.  
doi: 10.1016/j.actaastro.2012.03.026
- [11] A.V. Krivov, J. Getino, Orbital evolution of high-altitude balloon satellites, *Astronomy and Astrophysics*, 318, pp. 308-314, 1997.
- [12] A. V. Krivov, L. L. Sokolov, and V. V. Dikarev, "Dynamics of Mars-orbiting dust: Effects of light pressure and planetary oblateness," *Celestial Mechanics and Dynamical Astronomy*; Vol. 63, No. 3, pp. 313-339, 1995.  
doi: 10.1007/bf00692293
- [13] C. Colombo, C. Lücking, C.R. McInnes, "Orbital Dynamics of High Area-to-Mass Ratio Spacecraft under the Influence of  $J_2$  and Solar Radiation Pressure", submitted to *Acta Astronautica*, 2012.
- [14] R. Clark, "Residual Air Inflated System for Passive Deorbiting of CubeSats," MEng Aero-Mechanical Engineering Thesis. Department of Mechanical and Aerospace Engineering, University of Strathclyde, Glasgow, 2012.
- [15] R. Clark, *et al.*, University of Strathclyde, "StrathSat-R". REXUS Student Experiment Documentation, v1.0 (PDR), Glasgow, 2012.